Magneto-Electroacoustic Dynamics in a Straintronic Random Access Memory Cell

Vladimir Preobrazhensky, L.M. Krutyansky, Nicolas Tiercelin, Philippe Pernod

Magneto-Electroacoustic Dynamics in a Straintronic Random Access Memory Cell

V. L. Preobrazhensky[a,c], L. M. Krutyansky[a,c], N. Tiercelin[b,c], and P. Pernod[b,c]

a Prokhorov General Physics Institute, Russian Academy of Sciences, Moscow, Russia
b Univ. Lille, CNRS, Centrale Lille, ISEN, Univ. Valenciennes, UMR 8520 – IEMN, Lille, France
c Joint International Laboratory LIA LICS

Abstract
The straintronic principle of nonvolatile magnetoelectric random access memory (MELRAM) is attracting attention because of the prospect of achieving ultra-low-power consumption in memory devices on its basis. The mechanism of switching magnetic moments by pulse deformation of elastically coupled magnetic and piezoelectric subsystems is associated with the excitation of acoustic oscillations in memory cells. The oscillation period in nanoscale cells is comparable to the switching time of magnetic moments, which can distort the process of recording information. The influence of acoustic excitations on the dynamics of magnetic switching has been investigated using numerical simulation in relation to a magnetostrictive cell of 50 × 50 × 400-nm size on a PMN-PT ⟨011⟩ piezoelectric substrate. The parameters of the control electrical pulses providing stable binary switching of the system magnetic states have been determined.

Keywords:
piezoelectric–magnetic, impulse deformation, acoustic oscillations, magnetization switching.

Reducing energy consumption for writing and reading information is one of the key tasks of creating a new generation of random access memory devices [1]. The use of magnetoelectric interaction in natural multiferroics [2–5] or artificial multiferroic structures based on elastically coupled magnetostrictive and piezoelectric components appears to be a promising approach to solving the problem [6–10]. The control of magnetic states by means of electric fields in magnetoelectric memory cells (MELRAM) allows reducing the power consumption for information recording by up to tens of attojoules per bit [9]. In this case, the switching times determined by the magnetic resonance frequency and spin relaxation parameters are estimated at nanosecond fractions. Piezoelectric deformations in MELRAM cells are usually considered in a quasi-static approximation without taking into account hypersonic oscillations excited by control pulsed electric fields. At the same time, strain variables contribute to effective magnetostrictive fields that switch magnetic states and can introduce errors into recording processes. The role of oscillations is particularly significant if the frequency band of the control pulses covers the frequencies of the structure's own acoustic modes. In this paper, the elastic dynamics of the structure is included in the simulation of magnetoelectric switching of magnetization in a nanoscale MELRAM cell controlled by nanosecond and subnanosecond pulses of electric voltage. The elastic oscillations of the structure were calculated using the COMSOL Multiphysics software package. The results of this calculation were used to describe the magnetization switching processes in the numerical integration of the Landau–Lifshitz–Hilbert equation.

The geometry of the structure in question, which is shown in Fig. 1, is similar to the one proposed in [11] for a fully magnetoelectric cell, in which both recording and reading of information are carried out using pulsed electric fields. The size of the cell piezoelectric part is 75 × 500 × 200 nm. The role of the information carrier is performed by a 50 × 50 × 400-nm intermetallic magnetostrictive film with uniaxial magnetic anisotropy applied on top of the piezoelectric and placed in magnetic field **H** oriented at an angle of 45° to the *y* axis in the plane of the film. The orientation of the easy magnetization axis in the plane is chosen so that to ensure equality of the energies of two stable equilibrium states "0" and "1" with magnetization directions along the *x* or *y* axis, respectively. In this case, angle α between the easy and *x* is determined, taking into account the shape anisotropy, by the ratio of the transverse demagnetizing field to the magnetic anisotropy field: $\cos 2\alpha = H_m/H_A$. The equilibrium orientations of the magnetization along the *x* and *y* axes are achieved under the condition $H = H_A^{\text{eff}}/\sqrt{2}$, where the magnetic anisotropy effective field is equal to $H_A^{\text{eff}} = H_A\sqrt{1-(H_m/H_A)^2}$.

The piezoelectric substrate is represented in the calculations by a fragment of a size of 1000 × 1300 × 1200 nm. In the numerical model, the selected fragment is surrounded by a sound-absorbing layer along the perimeter in order to avoid spurious reverberation. The intermetallic magnet also plays the role of the upper electrode in addition to the main function of the information carrier. The lower electrode is located on the substrate around the cell. The impulse voltage applied to the electrodes creates an anisotropic $\langle u_{xx} - u_{yy} \rangle$ strain in the structure, which controls the magnetization switching. The voltage polarity uniquely determines the resulting orientation of the magnetization "0" or "1" independently of the initial magnetic state.

The results of the calculation of the $\langle u_{xx} - u_{yy} \rangle$ strain averaged over the volume of the magnetostrictive film obtained using the COMSOL Multiphysics package are presented in Fig. 2. The Young's modulus, Poisson's ratio, and film density were assumed to be E = 126 GPa, v = 0.345, and p = 9600 kg/m^3, respectively. The crystal $Pb(Mg_{1/3}Nb_{2/3})O_3$–$PbTiO_3$ (PMN-PT) of the ⟨011⟩ cut was considered as a piezoelectric, the full set of parameters of which is given in [12]. The calculation was carried out for acoustic q-factor of materials Q = 1000. The amplitude of the voltage pulses was U_i = 0.2 V. The results shown in Figs. 2a and 2b were obtained for the electric pulse durations (level 0.5 of the maximum) equal to t_i = 0.27 and 1.96 ns, respectively, with the same front duration of 0.25 ns. The figures show the oscillations caused by resonant acoustic oscillations in the cell. The oscillation frequency does not change when the substrate is removed from the model. The emission of acoustic waves into the substrate increases the attenuation of the oscillations. It can be seen that the amplitude of the second (reverse) half- period of oscillations in Figs. 2a and 2b is about 45% of the average value during the action of the voltage pulse.

The strain calculation data were used to describe the magnetization switching process using the Landau–Lifshitz–Hilbert equation

$$\frac{\partial \mathbf{M}}{\partial t} = -\gamma \mathbf{T} + \frac{\delta}{M}\left[\mathbf{M} \times \frac{\partial \mathbf{M}}{\partial t}\right], \quad (1)$$

where T is the torque, γ is the magnetomechanical ratio, and δ is the attenuation coefficient. In angular variables, which determine the projection of the magnetic moment in the coordinate system (ξ, η, ζ) associated with the direction of magnetizing field η || H, ζ || z, M_ξ = Mcosθsinϕ, M_η = Mcosθcosϕ, and M_ζ =Msinθ, where angle θ is counted from the plane of the film, Eq. (1) is converted to the form

$$\begin{aligned} \frac{\partial \varphi}{\partial t} &= -\frac{\gamma}{M\Delta}[T_\xi \cos\theta + T_\varsigma(\sin\theta \sin\varphi - \delta\cos\varphi)], \\ \frac{\partial \theta}{\partial t} &= -\frac{\gamma}{M\Delta}[T_\xi \delta \cos^2\theta + T_\varsigma(\cos\theta\cos\varphi \\ &\quad + \delta \sin\theta\cos\theta\sin\varphi)], \end{aligned} \quad (2)$$

Where = $(1 + \delta^2)\cos^2\theta\cos\phi$,

$$\begin{aligned} T_\xi/M &= \frac{1}{4}(H_A^{\text{eff}} - H_A - H_m)\sin 2\theta\cos\varphi - H\sin\theta \\ &\quad + \frac{B}{2M}\langle u_{xx} - u_{yy}\rangle \sin 2\theta \sin\varphi, \\ T_\varsigma/M &= -\frac{1}{2}H_A^{\text{eff}}\cos^2\theta\sin 2\varphi + H\cos\theta\sin\varphi \\ &\quad + \frac{B}{M}\langle u_{xx} - u_{yy}\rangle \cos^2\theta\cos 2\varphi. \end{aligned} \quad (3)$$

Here, B is the magnetostriction constant. Figures 3a and 3b present the results of solving Eqs. (2) with variable $\langle u_{xx} - u_{yy} \rangle$ strains, which are shown in Figs. 2a and 2b, respectively. The initial equilibrium state is $\phi = \pi/4$ and $\theta = 0$. The calculation was performed in relation to the nanostructured N ($TbFe_2$/FeCo) film (N is number of bilayers) with giant magnetostriction (B = 10 MPa) and magnetic parameters M = 200 emu/cm^3, H_A = 1.3 kOe, and $\delta = 0.15$. The inserts in Figs. 3a and 3b show phase por- traits of the magnetization oscillations $\theta(\phi)$.

According to the calculation, the magnetization switching is realized when the electric voltage pulse duration is greater than $t_i \cong 0.32$ ns, whereas the magnetic relaxation time is about 1 ns. Note that the calculation gives the value of control pulse minimum duration $t_i = 0.25$ ns at the same amplitude U_i = 0.2 V for the quasi-static approximation, which does not consider acoustic excitations. For duration t_i = 0.27 ns, the calculation shows a dynamic magnetization deviation from the orientation "0" followed by relaxation to the initial state (Fig. 3b).

An example of switching "0"–"1" for t_i = 1.96 ns and U_i = 0.2 V is shown in Fig. 3a. The minimum voltage amplitude that provides switching of magnetization at a given pulse duration is U_i = 70 mV as opposed to U_i = 46 mV in the quasi-static approximation. At the voltage of the opposite sign, there is no switching for any pulse durations, which confirms the unambiguous dependence of the final state of the magnetic system on the polarity of the control electric field.

The simulation of the process of switching magnetic states in a MELRAM magnetoelectric cell is performed using a structure that exhibits pronounced resonant excitations of acoustic vibrations accompanying applied pulsed electric fields. The oscillations impose additional restrictions on the minimum amplitude and duration of the control pulses compared to the results of the quasi-static approximation. Despite the considerable amplitudes of the variable components of strains at subnanosecond electrical stresses, the proper selection of the parameters of the control pulses ensures a stable switching of the magnetic states in the straintronic cell.

Funding:

This work was supported by the Russian Foundation for Basic Research, project no. 16-29-14022.

References:

1. *Nanomagnetic and Spintronic Devices for Energy-Effi- cient Memory and Computing*, Ed. by J. Atulasimha and S. Bandyopadhyay, 1st ed. (Wiley, Hoboken, NJ, 2016).
2. X.Chen, A.Hochstrat, P.Borisov,and W.Kleemann, Appl. Phys. Lett. **89**, 202508 (2006).
3. M.Bibes and A.Barthélémy, Nat.Mater.**7**,425(2008).
4. X. He, Y. Wang, N. Wu, A. N. Caruso, E. Vescovo, K. D. Belashchenko, P. A. Dowben, and C. Binek, Nat. Mater. **9**, 579 (2010).
5. A. A. Berzin, D. L. Vinokurov, and A. I. Morosov, Phys. Solid State **58**, 2320 (2016).
6. N. Tiercelin, Y. Dusch, A. Klimov, S. Giordano, V. Preob- razhensky, and P. Pernod, Appl. Phys. Lett. **99**, 192507 (2011).https://doi.org/10.1063/1.3660259
7. Y.Dusch,N.Tiercelin,A.Klimov,S.Giordano,V.Preob- razhensky, and P. Pernod, J. Appl. Phys. 113, 17C719 (2013). https://doi.org/10.1063/1.4795440
8. H. Ahmad, J. Atulasimha, and S. Bandyopadhyay, Sci. Rep. **5**, 18264 (2015). https://doi.org/10.1038/srep18264
9. S.Giordano,Y.Dusch,N.Tiercelin,P.Pernod,and V. Preobrazhensky, Phys. Rev. B **85**, 155321 (2012).
10. K. Y. Camsari, R. Faria, O. Hassan, B. M. Sutton, and S. Datta, Phys. Rev. Appl. **9**, 044020 (2018).
11. V.Preobrazhensky,L.Krutyansky,N.Tiercelin,Y.Dusch, A. Sigov, P. Pernod, and S. Giordano, Ferroelectrics **532**, 160 (2018). https://doi.org/10.1080/00150193.2018.1499403
12. F. Wang, L. Luo, D. Z. X. Zhao, and H. Luo, Appl. Phys. Lett. **90**, 212903 (2007).

Figures:

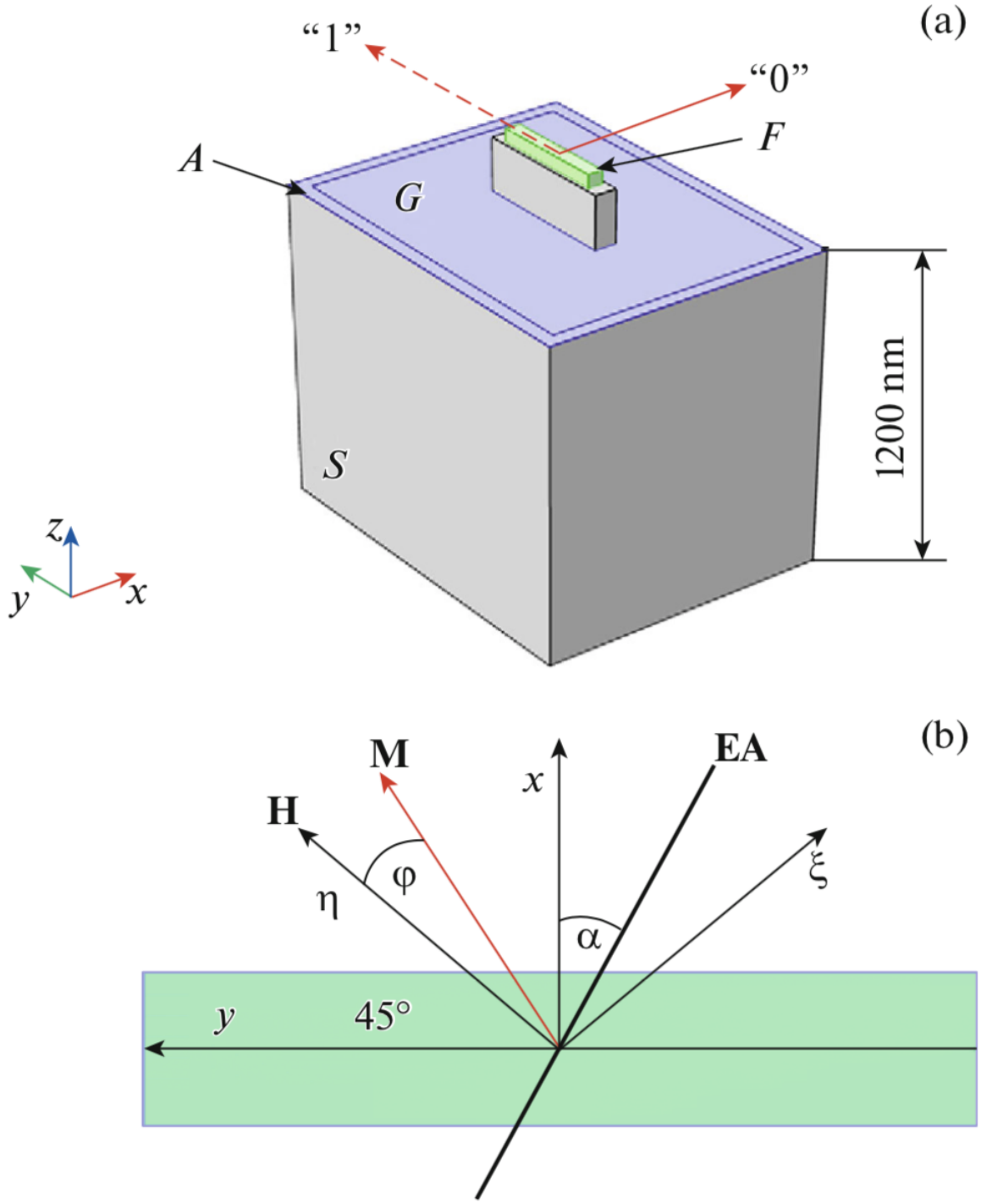

Fig. 1. Model of MELRAM cell on PMN-PT ⟨011⟩ substrate. (a) The geometry of the cell. *S* is a substrate with PMN-PT active cell located on it, *F* is a magnetostrictive intermetallic film, *G* is an electrode, and *A* is a virtual sound-absorbing layer. The magnetization directions corresponding to the "0" and "1" states are indicated. (b) The mutual orientation of the "easy axis" of magnetic anisotropy **EA**, magnetization vectors **M**, and magnetizing field **H** in the plane of the magnetostrictive film.

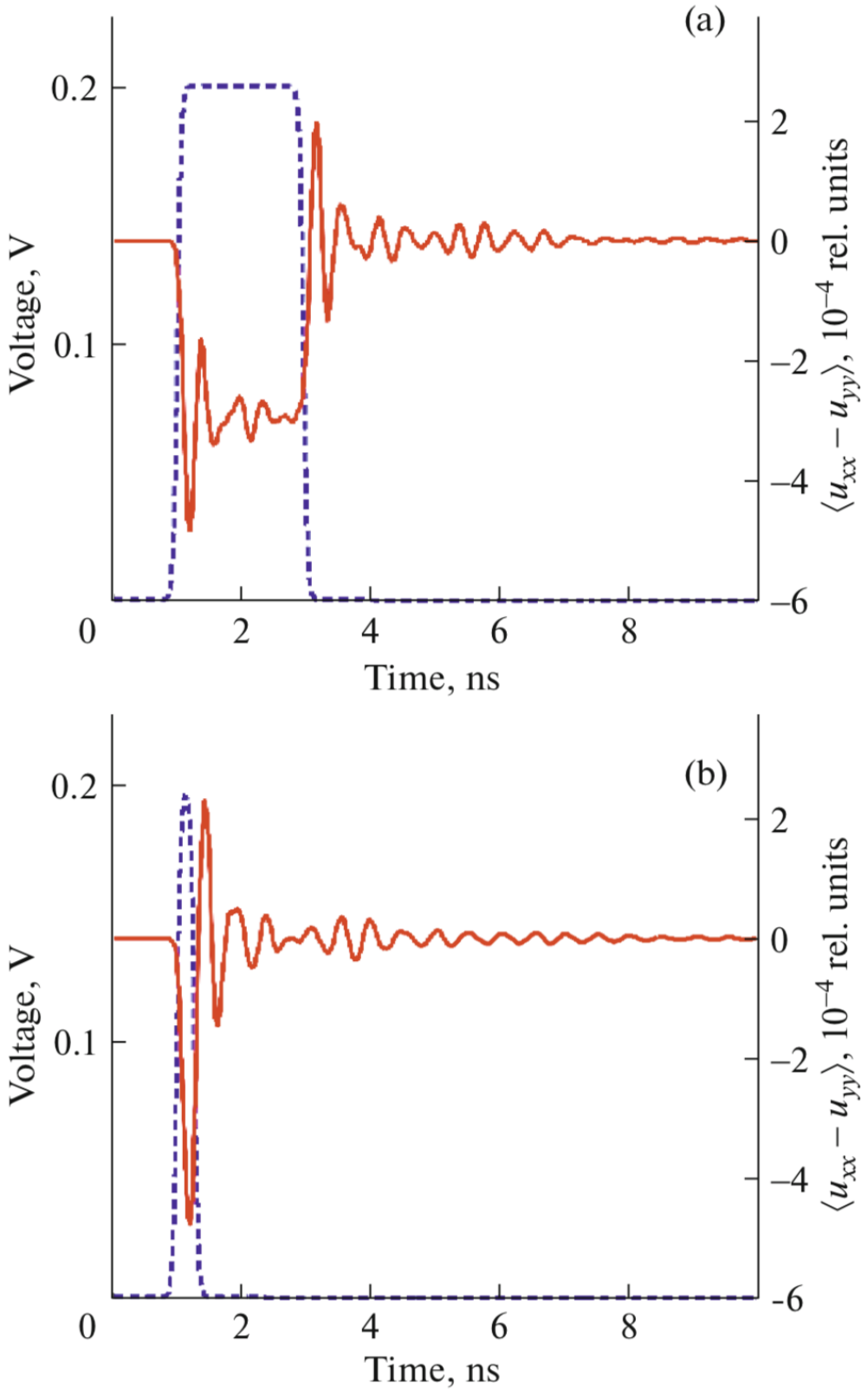

Fig. 2. Time dependence of the $\langle u_{xx} - u_{yy} \rangle$ strains averaged over the film volume (solid lines) for the pulses of the con- trol voltages with amplitude U_i = 0.2 V and duration t_i = (a) 1.96 and (b) 0.27 ns (dashed lines).

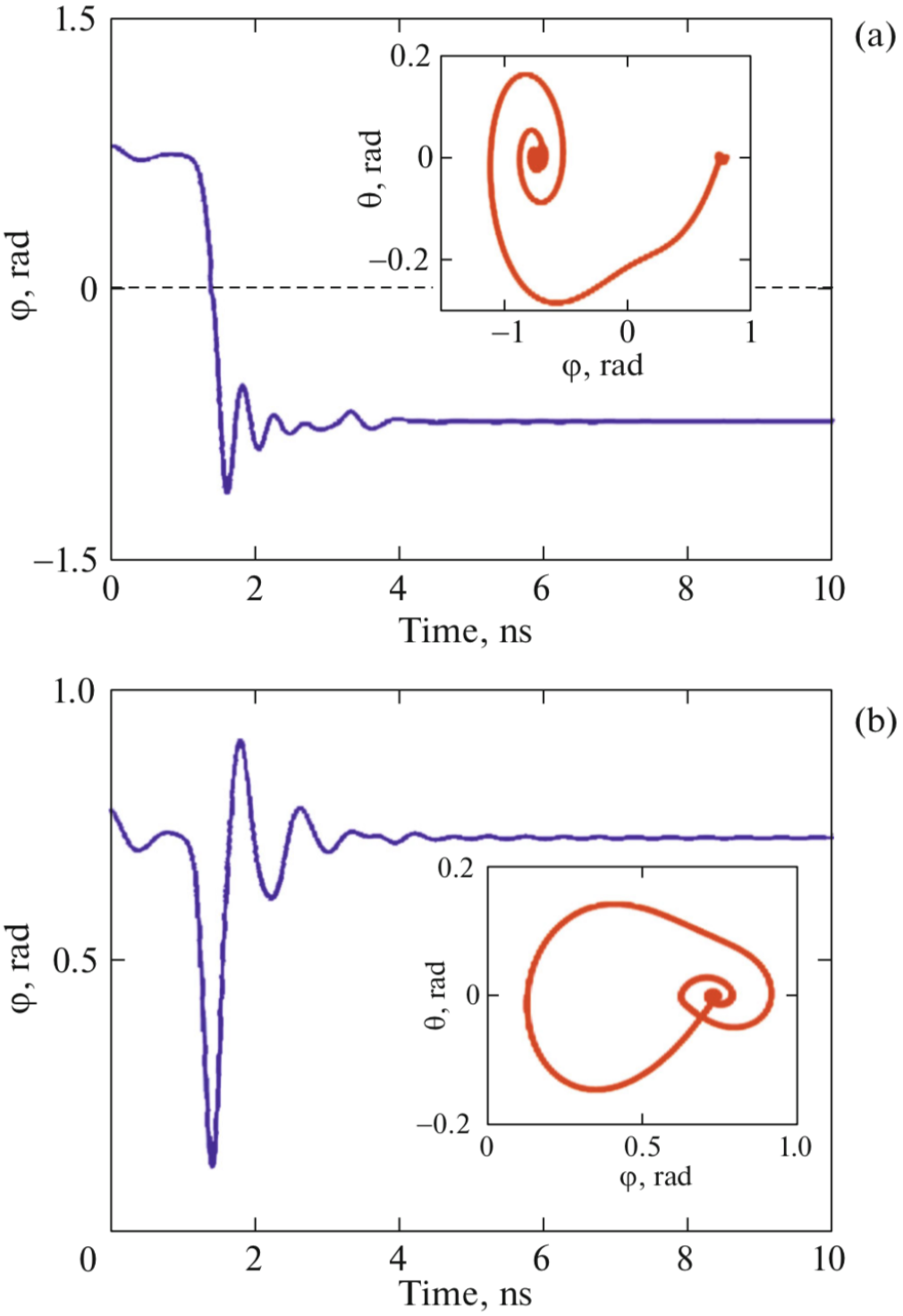

Fig. 3. Time dependence of angle φ between the magnetic moment and magnetizing field at control pulse durations t_i = (a) 1.96 and (b) 0.27 ns. The inserts show phase portraits θ(ϕ) of the magnetization movement (a) in the switching mode and (b) in the absence of switching of the magnetic states.